THE LATTICE WITH IMAGINARY γ-TRANSITION FOR THE CERN PROTON SYNCHROTRON PS2

Yu. Senichev*, Institute of Nuclear Physics, FZJ, Germany, D-52425, Juelich, Germany

Abstract

At present the new proton synchrotron PS2 with the energy range 4-50 GeV is discussed to upgrade LHC injector's complex [1]. Two lattices with and without the transition energy crossing are considered. In second option the momentum compaction factor must be kept low enough or negative. On the basis of the theory of "resonant" lattices for synchrotrons with complex transition energy developed in [2], the lattice with imaginary gamma-transition γ_{tr} for construction of PS2 lattice is proposed. Additionally the lattice should meet a number of important requirements, e.g., dispersion-free straight sections, a flexible scheme of chromaticity correction, a large enough dynamic aperture, etceteras.

INTRODUCTION

Since the longitudinal oscillation frequency is proportional to a root square of the slip factor $\eta = 1/\gamma_{tr}^2 - 1/\gamma^2$, the longitudinal stability at the transition $\gamma = \gamma_{tr}$ is lost. Therefore the acceleration through transition is considered a major problem, and the momentum compaction factor $\alpha = 1/\gamma_{tr}^2$ is one of the most important characteristics of any synchrotron. With regard to this problem, many methods have been developed for crossing the transition energy with minimum particle loss. However, in a high-intensity proton accelerator, the transition-energy crossing must be completely avoided because of the need for extremely low losses at the $10^{-3} - 10^{-4}$ level. Moreover, the slip factor should be as high as possible in order to increase the collective instability threshold. Besides the absolute value of slip factor can be used as additional factor for matching between two accelerators or/and control of beam sizes during acceleration.

To eliminate the transition energy crossing in anew designed PS2 synchrotron the gamma-transition must be moved away from acceleration range $\gamma \approx 5 \div 50$. For this purpose we use the theory of "resonant" lattices. With specially correlated modulation of quadrupoles gradient and orbit curvature and a particular choice of betatron oscillation frequencies, the theory of "resonant" lattices developed in [2] makes it possible to get interrelated dispersion variations D(s) and $1/\rho(s)$ along the equilibrium orbit and a negative momentum compaction factor

$$\alpha = \frac{1}{C}\oint^{C} \frac{D(s)}{\rho(s)} ds \le 0 \qquad (1)$$

A lattice like this should eliminate transition energy crossing by accelerated particles since the transition energy takes imaginary values $\gamma_{tr} = -i/\sqrt{|\alpha|}$. In addition, the PS2 lattice must meet a number of physical and technical requirements, such as independent tuning of the momentum compaction factor and betatron frequencies of arcs, zero dispersion in straight sections, effective chromaticity correction by the smallest possible number of quadrupole families, a large dynamic aperture. The latter implies first of all mutual compensation of the nonlinear effect of chromatic sextupoles on the motion of particles in the accelerator in the first order of the perturbation theory.

In this article we propose the imaginary γ_{tr} lattice for PS2 complying with the above conditions and discuss which lattice is optimal in view of the possible technological features of a particle accelerator.

The "resonant" lattice was first proposed for the Moscow Kaon Factory [3]. This lattice was then adapted for the TRIUMF KAON Factory (Canada) [4]. Later it was considered as the best candidate for the Superconducting Super Collider (SSC) Low Energy Booster (USA) [5], then was adopted for the main accelerator of the Neutrino Factory at CERN (Switzerland) [6], and ultimately was implemented in the JPARC (Japan Protons Accelerator Research Center), accelerator complex [2,7]. In the High Energy Storage Ring (HESR) lattice of the FAIR project, the same idea is also accepted [8].

The distinguishing features of this lattice are:

- ability to achieve the negative momentum compaction factor using the resonantly correlated curvature and gradient modulations;
- gamma transition variation in a wide region from $\gamma_t \approx \nu_x$ to $\gamma_t \approx i\nu_x$ (ν_x is the horizontal tune) with quadrupole strength variation only;
- dispersion-free straight section;
- independent optics parameters of arcs and straight sections;
- two families of focusing and one of defocusing quadrupoles;
- separated adjustment of gamma transition, horizontal and vertical tunes;
- convenient chromaticity correction method using sextupoles;
- first-order self-compensating scheme of multipoles and a large dynamic aperture;
- low sensitivity to multipole errors.

Hereinafter we will denote the horizontal tune ν_x as ν, since the vertical tune does not affect on the momentum compaction factor.

* On leave from Institute for Nuclear Research, RAS, Moscow, e-mail: y.senichev@fz-juelich.de

MAIN PROPOSITIONS OF THE "RESONANT" LATTICE THEORY

General principles of construction of "resonant" lattices detailed in [2] are based on the solution of the equation for the dispersion D(s) in the biperiodical structure.

$$\frac{d^2D}{ds^2}+[K(s)+\varepsilon\, k(s)]D=\frac{1}{\rho(s)} \qquad (2)$$

Here the gradient G(s) and the orbit curvature ρ(s) related to each other through the functions

$$K(s)=\frac{eG(s)}{p},\ \varepsilon\, k(s)=\frac{e\Delta G(s)}{p},$$

where $p=m_0\gamma v$ is the particle momentum, should be modulated resonantly and in correlation with each other.
In what follows we will use harmonics of the modulated function of gradients

$$\varepsilon\cdot k(\phi)=\sum_{k=0}^{\infty} g_k\cos\ k\phi \qquad (3)$$

where

$$g_k=\frac{e}{p}\cdot\frac{1}{\pi}\int_{-\pi}^{\pi}\Delta G\cos k\phi\, d\phi$$

is the k-th harmonic of the Fourier series of gradients function and

$$\phi=2\pi\cdot s/L_s$$

is the longitudinal coordinate normalized to the superperiod length L_s, and harmonics in the expansion of the curvature function

$$\frac{1}{\rho(\phi)}=\frac{1}{\overline{R}}\left(1+\sum_{n=1}^{\infty} r_n\cos n\phi\right) \qquad (4)$$

where

$$r_n=\frac{\overline{R}}{\pi}\int_{\pi}^{-\pi}\frac{\cos n\phi}{\rho(\phi)}d\phi$$

is the n-th harmonic of the Fourier series of the orbit curvature function and

$$\overline{R}=L_s\cdot S/2\pi$$

is the average curvature radius of the equilibrium orbit in the superperiod, S is the total number of superperiods.
Since mirror symmetry of the superperiod is one of the conditions for the construction of the "resonant" lattice, expansions of the functions $\varepsilon\, k(\phi)$ and $1/\rho(\phi)$ in the Fourier series involve only terms with cosines.
According to (1), the momentum compaction factor is the average value of the function $D(\phi)/\rho(\phi)$. In the general form, the dispersion $D(\phi)$ and the orbit curvature $\frac{1}{\rho(\phi)}$ can be represented in terms of the averages $\overline{D}$ and $\overline{R}$ and the functions $\tilde{D}(\phi),\tilde{r}(\phi)/\overline{R}$ oscillating about these averages:

$$D(\phi)=\overline{D}+\tilde{D}(\phi)\ \text{ and }\ \frac{1}{\rho(\phi)}=\frac{1}{\overline{R}}(1+\tilde{r}(\phi)).$$

Then the momentum compaction factor can be written as the sum

$$\alpha=\frac{\overline{D}}{\overline{R}}+\frac{\overline{\tilde{D}(\phi)\cdot\tilde{r}(\phi)}}{\overline{R}} \qquad (5)$$

In an ordinary regular FODO lattice without gradient and orbit curvature modulation the oscillating components are equal to zero, $\tilde{D}(\phi)=0$, $\tilde{r}(\phi)=0$, and the momentum compaction factor is governed by the first term in (5). Considering that the average dispersion in classical lattices is

$$\overline{D}=\frac{\overline{R}}{\nu^2}$$

we find that the minimum value of the momentum compaction factor

$$\alpha=\frac{\overline{D}}{\overline{R}}=\frac{1}{\nu^2}$$

is limited by the total number of horizontal betatron oscillations ν in the magnetic optical structure of length $S\cdot L_s$. In the "resonant" lattice, the functions of gradients and/or orbit curvature can be modulated jointly or individually. In [2] general expressions were obtained for the momentum compaction factor for one superperiod

$$\alpha_s=\frac{1}{\nu^2}\left\{1+\frac{1}{4}\left(\frac{\overline{R}}{\nu}\right)^4\sum_{k=-\infty}^{\infty}\frac{{g_k}^2}{(1-kS/\nu)[1-(1-kS/\nu)^2]^2}\right.$$
$$+\frac{1}{4}\sum_{k=-\infty}^{\infty}\frac{r_k^2}{1-kS/\nu}-\frac{1}{2}\left(\frac{\overline{R}}{\nu}\right)^2\sum_{k=-\infty}^{\infty}\frac{r_k g_k}{(1-kS/\nu)[1-(1-kS/\nu)^2]}$$
$$\left.-\frac{1}{2}\left(\frac{\overline{R}}{\nu}\right)^2\sum_{k=-\infty}^{\infty}\frac{r_k g_k}{[1-(1-kS/\nu)^2]}+O(g_k^i\cdot r_k^j, i+j\ge 3)\right\} \qquad (6)$$

and for the dispersion function maximum in a superperiod

$$D_{\max}=\frac{\overline{R}}{\nu^2}\hat{f}\cdot\left\{1-\frac{1}{2}\left(\frac{\overline{R}}{\nu}\right)^2\sum_{k=-\infty}^{\infty}\frac{g_k}{(1-kS/\nu)[1-(1-kS/\nu)^2]}\right.$$
$$\left.-\frac{1}{2}\left(\frac{\overline{R}}{\nu}\right)^2\sum_{k=-\infty}^{\infty}\frac{g_k}{[1-(1-kS/\nu)^2]}+\frac{1}{2}\sum_{k=-\infty}^{\infty}\frac{r_k}{1-kS/\nu}\right\}$$
$$+O(g_k^i\cdot r_k^j, i+j\ge 2) \qquad (7)$$

where kS is the modulation frequency of the k-th harmonic in the expansion of the gradient and curvature

functions, $\hat{f}$ is the function describing beam envelope oscillations, which is normalized to its average value. We will call the harmonic closest to ν (with the minimum possible difference $kS-\nu$) and producing the maximum effect on the momentum compaction factor the fundamental harmonic. This harmonic has kS oscillations over the entire lattice in question. In most cases under our consideration the frequency of the k-th harmonic coincides with the number of superperiods, i.e., k = 1 and $kS = S$. Indeed, if both the quadrupole gradient function and the orbit curvature function are modulated with an identical frequency (i.e., at k = n in (3) and (4)), the second term in (5) may make an appreciable contribution to the momentum compaction factor provided that the value $1-kS/\nu$ is small (see (6)).

In addition, from (6) there follows an obvious condition of antiphase modulation of the gradient and curvature function, which allows correlated variation of the momentum compaction factor with the aid of these functions. We call this lattice, based on the resonant and correlated perturbation of the magnetic optical channel parameters, the "resonant" lattice.

Thus, the following principles underlie the general approach to construction of a "resonant" lattice:

- the fundamental modulation frequency should be identical for the functions of the gradients and the orbit curvature and higher than the horizontal betatron frequency $kS > \nu$ with as minimum a difference $kS-\nu$ as possible;
- modulation of the orbit curvature should be in antiphase with modulation of the quadrupole gradients, $g_k r_k < 0$;
- amplitudes of each of the fundamental harmonics, g_k and r_k, should be as high as possible;
- exact equality of the frequencies $\nu = kS$ and $\nu = kS/2$ at which the dispersion and the β-function increase beyond limits should be eliminated.

A SUPERPERIOD OF THE "RESONANT" LATTICE

In common case there are two types of lattices used in accelerators with inserted straight sections, the so-called circular lattices with S identical superperiods and the lattice consisting of arcs with S_{arc} superperiods per each one separated by straight sections. In the former lattices the momentum compaction factor completely coincides with its value for one superperiod. In the lattices consisting of arcs with S_{arc} superperiods of length L_s and separated by straight sections of length L_{str}, the momentum compaction factor for the entire accelerator α_{total} and for a superperiod α_s are related by the equation

$$\alpha_{total} = \alpha_s \frac{S_{arc} \cdot L_s}{S_{arc} \cdot L_s + L_{str}}. \qquad (8)$$

Thus, knowing the momentum compaction factor for one superperiod, one can easily find its value for the entire accelerator.

For the proton synchrotron PS2 the racetrack lattice was adopted due to many reasons considered in [1]. On the straight sections several injection and extraction systems must be implemented [9]. Since the straight sections do not affect essentially on the momentum compaction value, just as a coefficient in expression (8), we concentrate our investigations on the arc structure for the most part. So, hereinafter we discuss the arcs structure only, assuming they can be easily matched with the designed straight sections. For the dynamic aperture calculation we take the straight section as regular FODO insertions between arcs.

The arcs are based either on the regular cell-periodical structure or on superperiods. A superperiod is usually formed by varying parameters of a regular lattice consisting of singlet FODO cells, doublet FDO cells, or triplet FDFO cells (F is the focusing quadrupole, D is the defocusing quadrupole, and O is the drift space), each having its advantages and drawbacks. However, considering the chromaticity compensation requirement, the FODO lattice is most preferable because the other two lack good separation of the horizontal and vertical β-functions, which results in a decreased efficiency of the sextupoles and accordingly in a decreased dynamic aperture. In addition, the FODO superperiod with mirror symmetry about its centre provides most favourable conditions for independent control of the betatron frequencies, chromaticity in both planes, and momentum compaction factor, which makes a lattice like this superior to any other.

The number of cells in a superperiod N_{cell} is dictated by the required phase advance of radial oscillations. Following the theory of resonant lattices, we will try to construct a lattice with the horizontal frequency ν_{arc} as close to the number of superperiods S_{arc} as possible [2]. In this case, the phase advance of horizontal oscillations per cell will be about $2\pi \frac{\nu_{arc}}{S_{arc} \cdot N_{cell}}$. At the same time it is known that from the point of view of minimization of the β-functions for a cell the phase advance of radial oscillations should fall within the range 60°–100°. Thus, in a lattice with the fundamental harmonic of the modulation of the superperiod parameters k = 1 and with $\nu_{\text{arc}} < S_{arc}$ the number of cells turns out to be 3–5 per superperiod.

Since an increase in the number of cells requires greater splitting of the superperiod and entails an increase in the number of magnetic optical elements, we exclude the five-cell option from consideration and confine ourselves to analysis of a superperiod comprising 3–4 cells.

Figures 1and 2 show the behavior of the function $\beta_{x,y}$ and D_x in a regular arc based on plain FODO cells, where each drift space accommodates a bending magnet. Taking into account the PS2 parameters [1], the magnetic rigidity

$p/e \approx 170\ m{\cdot}T$, the cells number 22, the maximum field in magnet 1.8 T and the maximum gradient in quadrupole

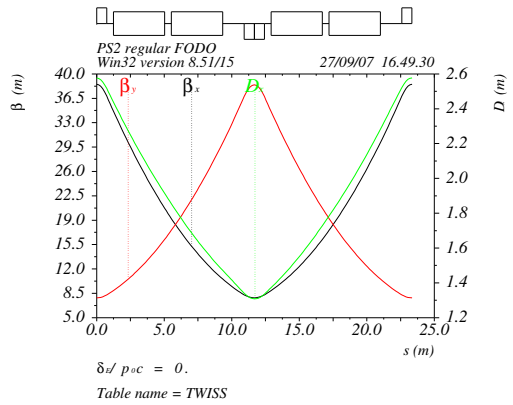

Figure 1: FODO cell

17 T/m the arc total length together with two missing magnet suppressors at edges is to be 513.5 m. Obviously, strict periodicity of cells does not make it possible to get the required value of the momentum compaction factor which is fixed by the value of the horizontal betatron frequency in this case $\gamma_{tr} \approx 10$.

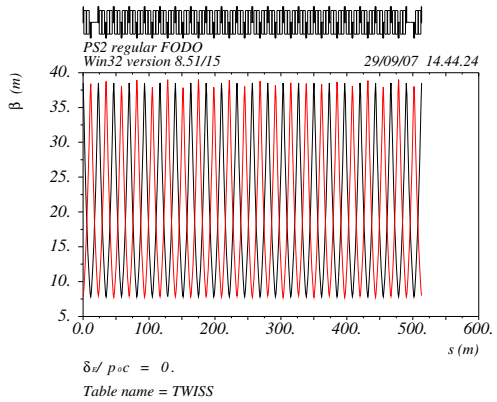

Figure 2: Arc based on FODO with dispersion suppressors located at edges of arcs

As a remark to make the gamma-transition higher than 50 the total number of FODO cells has to be increased up to 110 per arc. Therefore the only possible solution to eliminate the gamma-transition crossing is the "resonant" lattice.

Figure 3 shows a superperiod made up of three FODO cells with gradient modulation alone and mirror symmetry about the center, where two quadrupole families form the required fundamental harmonic $k = 1$. The arc is supposed to consist of 8 superperiods with the same total length of arc 513.5 m. However, to get the required gamma-transition $\gamma_{tr}=i10$ [1] this modulation method requires a great change of the field in the quadrupoles. Note that strong modulation of the gradients leads to a considerable increase in β-functions, in our case $\beta_x \sim 100$ m, and chromaticity of the entire accelerator, which results in a reduced dynamic aperture, and therefore this version of the resonant lattice is left out of consideration.

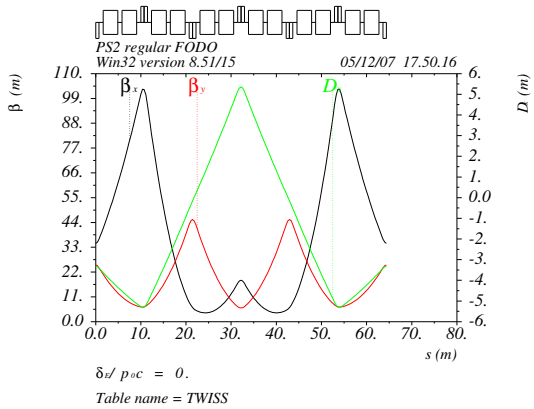

Figure 3: Superperiod with gradient modulation

Figure 4 correspond to the lattices where a superperiod is made up of three cells and the fundamental harmonic $k = 1$ is produced by modulation of the orbit curvature through using empty central cells called missing magnets (or missing magnet cells). In these curvature-varying lattices β-functions became smaller and chromaticity is kept lower. But unfortunately, the orbit curvature modulation method does not always provide the required value of gamma-transition. In our case under arc length restricted by 513.5 m it is about $\gamma_{tr} \approx 12$, which one is absolutely not enough.

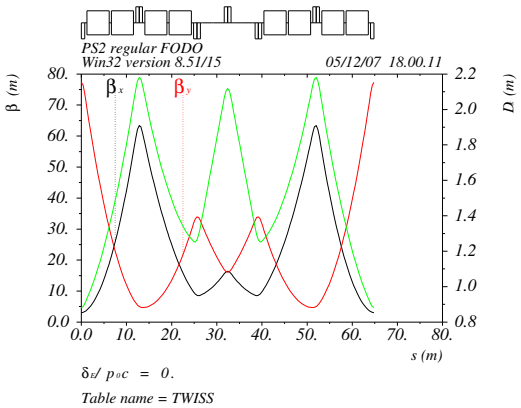

Figure 4: Superperiod with orbit curvature modulation

Thus, modulation of the orbit curvature and modulation of the quadrupole gradients can be used to get the required momentum compaction factor. The former method allows controlling the momentum compaction factor with the minimum increase in the β_x function and D_x and, compared with gradient modulation lattices, does not require strong sextupoles for chromaticity correction. However, the gradient modulation method is more flexible as it allows the momentum compaction factor of the already existing machine to be varied. In addition, it is often impossible to employ the factor $1/(kS_{arc}/\nu_{arc} - 1)$

and to increase it by making ν_{arc} approach kS_{arc}, which results in ineffectiveness of each method used separately. For example, in high-intensity accelerators one of the requirements is zero dispersion in straight sections. This means that the phase advance of radial oscillations in arcs should be a multiple of 2π and the condition $\min\{kS_{arc} - \nu_{arc}\} = 1$ should hold.

Based on the above reasoning, the "resonant" lattice method with simultaneous orbit curvature and quadrupole gradient modulation with an identical frequency of the fundamental harmonics and an approximately identical contribution of both modulations to the final value of the momentum compaction factor is most effective. From (6) it is easy to derive the following equality for an arbitrary fundamental harmonics g_k and r_k giving $\alpha \approx -1/\nu^2$:

$$\left(\frac{R}{\nu}\right)^2 \cdot \frac{g_k}{1-\left(1-kS_{arc}/\nu_{arc}\right)^2} - r_k = \pm 2^{3/2}\left(kS_{arc}/\nu_{arc} - 1\right)^{1/2}$$

and (9)

$$|r_k| \le \left(\frac{R}{\nu}\right)^2 \left|\frac{g_k}{1-(1-kS_{arc}/\nu_{arc})^2}\right|$$

As was already mentioned, modulation of gradients and modulation of the orbit curvature should be in antiphase and the reasonable location of the missing magnet cell is at the centre of the superperiod. This means that the amplitude of the fundamental harmonic of the orbit curvature modulation should be negative, $r_n < 0$, and therefore the amplitude of the gradient modulation will be positive. At these conditions the gamma-transition varies in a wide region from $\gamma_{tr}=\nu$ to $\gamma_{tr}=i\nu$ with quadrupole gradient modulation only. As an example of a lattice with both modulations, you can see figure 5.

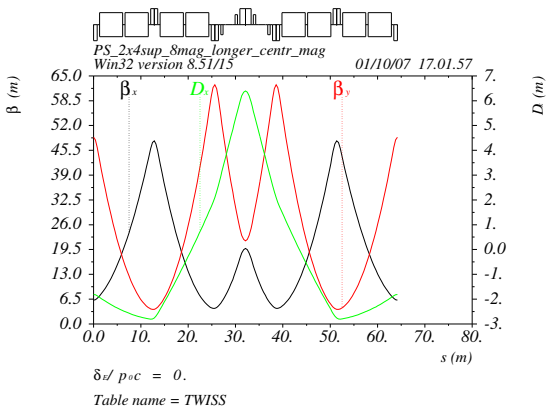

Figure 5: Superperiod of "resonant" lattice with simultaneous orbit curvature and quadrupole gradient modulation

However under the PS2 arc length restriction 513.5 m the central drift has to be shorter, and the zero momentum compaction factor can be obtained with additional modulation of gradients at a level of approximately 20% (see Fig. 6). In result the horizontal β_x-function on 10 % above in comparison with regular structure.

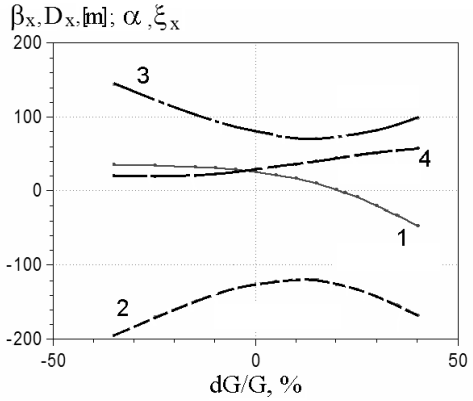

Figure 6: The α (1), ξ_x (2), β_x (3) and D_x (4) versus the gradient modulation

Figures 7 and 8 show the results yielded by various modifications of the method. In the first case (Fig. 7) the central quadrupole is "cut" in two slices and a sextupole is inserted between the slices, as was done, for example, in the JPARC project [7].

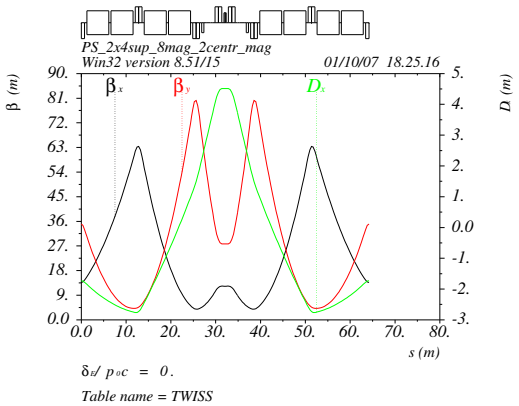

Figure 7: Superperiod with the central quadrupole sliced

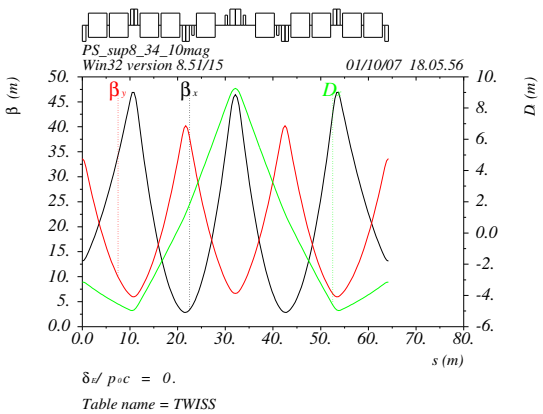

Figure 8: Superperiod with 10 magnets

On the one hand, positioning of the sextupole at a point where the horizontal β-function has a large value

increases its efficiency and thus the total number of focusing sextupoles can be reduced. On the other hand, division of a quadrupole into two halves increases their number. To our mind, this design does not give any significant advantages and is only a modification of the universally accepted resonant lattice. In the second case (Fig. 8) the orbit curvature is varied without a decrease in the total number of magnets, by varying the central cell length alone. This option may be advantageous for a magnetic optical lattice with rectangular magnets because the magnet sagitta is considerably decreased.

STRUCTURE OF ARCS

Now let us consider the magnetic optical structure of the entire accelerator, i.e., lattices of its arcs and straight sections. The straight sections will be added as the FODO insertions between arcs without details, since their structure do not affect on the momentum compaction factor and is specified and designed in [9]. Considering that physics equipment is to be installed in straight sections, let us formulate additional requirements to the resonant lattices:

- independent tuning of arcs and straight sections;
- controllable variation of the momentum compaction factor within the range $\alpha \sim 1/\nu^2$ to $-1/\nu^2$;
- ability to correct chromaticity of the entire accelerator by sextupoles located in the arcs;
- a sufficiently large dynamic aperture with allowance for all nonlinearities;
- zero dispersion in straight sections.

The first condition determines the macrostructure of the accelerator, namely, separation in functions between arcs and straight sections. Arcs fulfill bending functions and functions governing the main magnetic optical characteristics of the lattice, such as the momentum compaction factor, suppression of chromaticity, zero dispersion in straight sections, and correction of higher-order nonlinearities. Straight sections fulfill functions associated with accommodation of experimental equipment and final tuning of betatron oscillation frequencies of the entire accelerator. In addition, the optics of the arcs should be independent of the optics of the straight sections to allow more convenient work and minimum preparation for experiments. The number of arcs and straight sections is dictated by many parameters, first of all by the required architecture of the ring and the projected experiments, and for the PS2 it is two [1,9].

For the dispersion in straight sections to be zero, the arc consisting of S_{arc} superperiods should have a phase advance of radial oscillations that is a multiple of 2π, i.e., ν_{arc} should be an integer. This means that the phase advance in one superperiod should be $2\pi\nu_{arc}/S_{arc}$. On the other hand, for the momentum compaction factor to be controlled, the betatron frequency of horizontal oscillations should be smaller than the number of superperiods multiplied by the number of the fundamental harmonic. From this point of view it is reasonable to take the minimum possible difference

$$\nu_{arc} - kS_{arc} = -1 .$$

Thus, there exist many ratios between S_{arc} and ν_{arc}:

(4:3), (6:5), (8:7), (10:9), ….

Besides, there is another possibility. The arc may be divided into an equal integral number of superperiods within which the above ratios hold, for example, the ratio can be

$$S_{arc} : \nu_{arc} = 8 : 6 = 2 \text{ x } (4:3)$$

Actually, the arc is divided into two arcs in the ratio 4 : 3 without a straight section, and the zero dispersion condition is met not only at the edges but also in the middle of this double arc. As is seen, in all ratios the number of superperiods S_{arc} is taken to be even while the betatron oscillation frequency takes on integral odd values. In this case, the phase advance of the radial oscillations between the cells located in different superperiods and separated by $S_{arc}/2$ superperiods is obviously

$$2\pi \cdot \frac{\nu_{arc}}{S_{arc}} \cdot \frac{S_{arc}}{2} = 2\pi \cdot \frac{\nu_{arc}}{2} = \pi + 2\pi n ,$$

which corresponds to the condition of first-approximation compensation for the nonlinear effects of sextupoles located in these cells. This remarkable property also applies to higher multipoles in bending magnets and quadrupoles because each of them has a partner in the other quarter of the arc at a distance of odd integral π of radial oscillations (see Fig. 9).

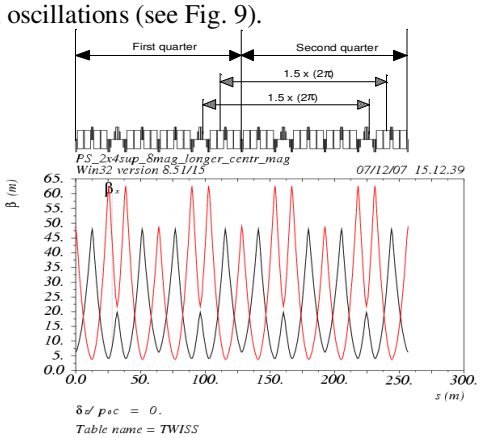

Figure 9: Half of arc with (S_{arc}:ν_{arc})=8:6

Thus, choosing S_{arc}, k, and ν_{arc}, we determine the lattice of the arc and the number of arcs. On the one hand, we are limited by strict rules for the choice of these parameters, on the other, the choice is quite wide and we may speak about a certain class of accelerators with such arcs.

By way of example, let us consider two versions of the lattice for the PS2 accelerator with an identical number of arcs and identical transition energy $\gamma_{tr} = i10$. In the first version the arc has the number of superperiods S_{arc} = 8

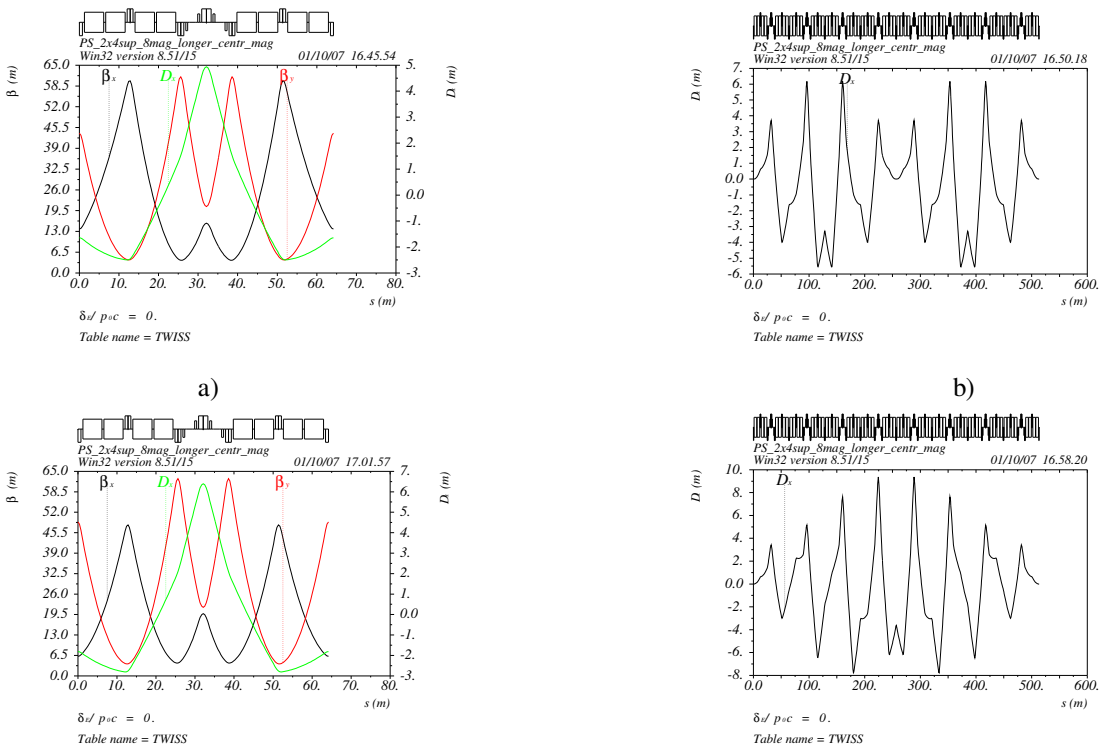

Figure 10: Dependence of the β-functions (a, c) in one superperiod and the dispersion (b, d) in the 8-superperiods arc with the horizontal tune ν_{arc}=6 (a, b) and ν_{arc}=7 (c, d) and 8 magnets per one arc.

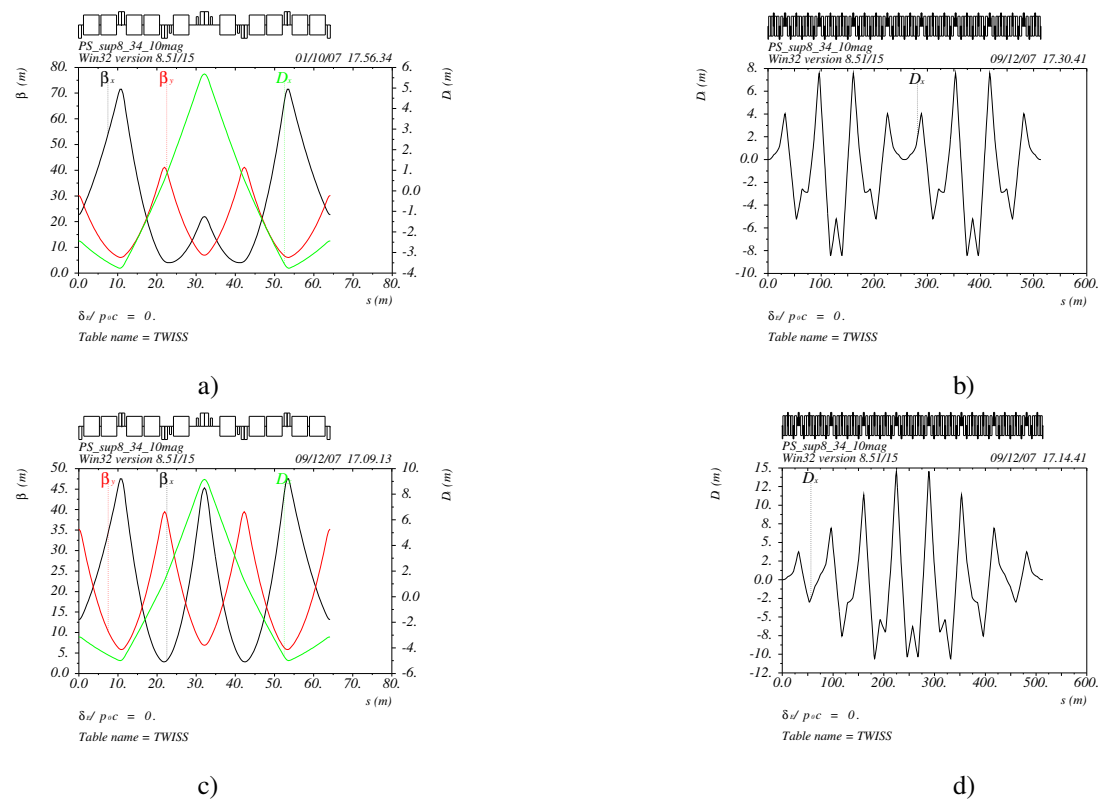

Figure 11: Dependence of the β-functions (a, c) in one superperiod and the dispersion (b, d) in the 8-superperiods arc with the horizontal tune ν_{arc}=6 (a, b) and ν_{arc}=7 (c, d) and 10 magnets per one arc.

Table 1: TWISS parameters of regular FODO lattice and "resonant" lattices with 8 superperiods per arc

Options(arc length=513.5 m)	γ_{tr}	$\beta_x$max	$\beta_y$max	$D_x$max
Regular lattice with 22 FODO cells (84 magnets per arc)	~10	39	39	3.5
Resonant lattice with ν_x=6; ν_y=6; longer central quadrupole, 8 magnets per superperiod	~i8÷10	60	61	6.2
Resonant lattice with ν_x=6; ν_y=6; two central quadrupoles; 8 magnets per superperiod	~i8÷10	62	69	6.0
Resonant lattice with ν_x=7; ν_y=6; longer central quadrupole; 8 magnets per superperiod	~i8÷10	48	62	9.4
Resonant lattice with ν_x=7; ν_y=6; two central quadrupoles; 8 magnets per superperiod	~i8÷10	49	71	9.0
Resonant lattice with ν_x=6; ν_y=6; longer central quadrupole; 10 magnets per superperiod	~i8÷10	71	41	7.9
Resonant lattice with ν_x=7; ν_y=6; longer central quadrupole; 10 magnets per superperiod	~i8÷10	47	40	14.5

Table 2: Magnito-optic elements of regular FODO lattice and "resonant" lattices with 8 superperiods on arc

One arc: length=513.5 m	N_{mag}	L_{mag}	N_{quad}	L_{quad}	N_{sext}	L_{sext}
Regular with 22 FODO cells (84 magnets per arc)	84	3.7	44	1.5	44	0.5
Resonant lattice with ν_x=6; ν_y=6; longer central quadrupole, 8 magnets per superperiod	64	4.9	48	1.5;2.3	32	0.5
Resonant lattice with ν_x=6; ν_y=6; two central quadrupoles; 8 magnets per superperiod	64	4.9	56	1.5	32	0.5
Resonant lattice with ν_x=7; ν_y=6; longer central quadrupole; 8 magnets per superperiod	64	4.9	48	1.5;2.3	32	0.5
Resonant lattice with ν_x=7; ν_y=6; two central quadrupoles; 8 magnets per superperiod	64	4.9	56	1.5	32	0.5
Resonant lattice with ν_x=6; ν_y=6; longer central quadrupole; 10 magnets per superperiod	80	3.9	48	1.5;2.3	32	0.5
Resonant lattice with ν_x=7; ν_y=6; longer central quadrupole; 10 magnets per superperiod	80	3.9	48	1.5;2.3	32	0.5

and the frequency of horizontal oscillation in the arc ν_{arc} = 6, in the second version S_{arc} = 8 and ν_{arc} = 7 (see Fig. 10). Besides, both versions have two options with 8 and 10 magnets per one superperiod (see Fig. 11). In tables 1 and 2 parameters of the considered structures are placed. In spite of all structures have identical properties, it is reasonable to take finally the structure with the minimal values of $\beta_{x,y}$ and D_x as optimum structure.

For the dispersion in the straight sections to be zero, the phase advance of radial oscillations should be a multiple of 2π and the dispersion should begin with the zero value at the entrance of the arc. Therefore, the dispersion oscillates with a double frequency: the superperiod frequency and the arc periodicity. This leads to an additional increase in the maximum dispersion in the arc. Obviously the longer arc, the bigger amplitude of second periodicity. For example, in the arc with S_{arc}: ν_{arc}=8:6 the dispersion increases from 6 m for superperiod to 8 m for arc, which is a ~30% increase, and in the arc with S_{arc}: ν_{arc}=8:7 the maximum dispersion increases from 6.5 m to 9.5 m correspondingly, which is a ~45% increase. In the latter case the arc period is longer and thus the arc periodicity causes a larger increase in dispersion. Note that in both cases the arc periodicity of the dispersion function does not lead to variation in the momentum compaction factor because integral (1) remains unchanged. The behavior of the $\beta_{x,y}$-functions also remains unchanged because the initial zero dispersion values do not affect them. Since arcs and straight sections are separated in functions, the betatron oscillation frequencies $\nu_{x,y}$ in the arcs do not change in any mode of operation and therefore quadrupoles specially inserted in the straight sections and providing the desired fraction value of the betatron frequency of the entire machine are responsible for the control of the working point position. However, in the case of retuning of the momentum compaction factor, the arc edge values of

the $\beta_{x,y}$-functions change. Therefore, special matching sections are inserted in the straight sections, which, with their four quadrupoles, allow matching of the arcs and straight sections to be retained. As a result, arcs are fully independent of straight sections and correction of the momentum compaction factor does not affect the values of the $\beta_{x,y}$-functions set for the straight section's facilities. If there are no special requirements to the behavior of the $\beta_{x,y}$-functions in the straight sections, the straight section lattice is usually mirror symmetrical about its middle, and therefore all quadrupoles of the straight sections can be directly used for matching arcs and straight sections. This considerably simplifies tuning of the entire accelerator due to minimization of the number of quadrupole families in the straight sections.

CONTROL OF MOMENTUM COMPACTION FACTOR AND ARCS TUNE

As we know in the "resonant" lattice in order to achieve the required momentum compaction factor, we modulate the quadrupole gradients on arcs correlated with a fixed orbit curvature modulation. In practice, we should know exactly which element controls the momentum compaction factor and arc tunes. Moreover, the element responsible for one function should be minimally correlated with the element responsible for another function. Due to the special features of the "resonant" lattice, this principle can be realized. From formulas (6) and (7), we can derive that at the mirror superperiod symmetry, the dispersion and the β functions are modulated by factors:

$$D(\phi) \propto \left\{1-\frac{1}{2}\left(\frac{\overline{R}}{\nu_{total}}\right)^2 \times \right.$$

$$\left. \frac{g_k \cos k\phi}{(1-kS_{arc}/\nu_{arc})[1-(1-kS_{arc}/\nu_{arc})^2]} + \frac{1}{2}\frac{r_k \cos k\phi}{1-kS_{arc}/\nu_{arc}} \right\}$$

$$\beta_{x,y} \propto \cos \mu\phi \left[1-\frac{1}{2}\left(\frac{\overline{R}}{\nu_{total}}\right)^2 g_k \frac{\cos k\phi}{1-(1-kS_{arc}/\nu_{arc})^2}\right] \quad (10)$$

On condition that ratios $kS_{arc} > \nu_{arc}$, $g_k > 0$ and $r_k < 0$ are fulfilled for the fundamental harmonic k=1, the maximum dispersion will be at the superperiod center $\phi = 0$, and the maximum horizontal β-function beginning at $\phi = -\pi$ and ending at $\phi = \pi$ on the superperiod.

Figure 12 shows the functional control of all quadrupoles. In the "resonant" lattice, the central focusing quadrupole QF2 is placed in the maximum dispersion giving it the main role in controlling the fundamental harmonic. Another focusing quadrupole QF1 is placed in the maximum β_x-function, which makes it effective at controlling the horizontal tune. Due to FODO features, the $\beta_{x,y}$ - functions are very well separated and two defocusing quadrupoles independently affect the vertical tune. To prove independent controllability of the momentum

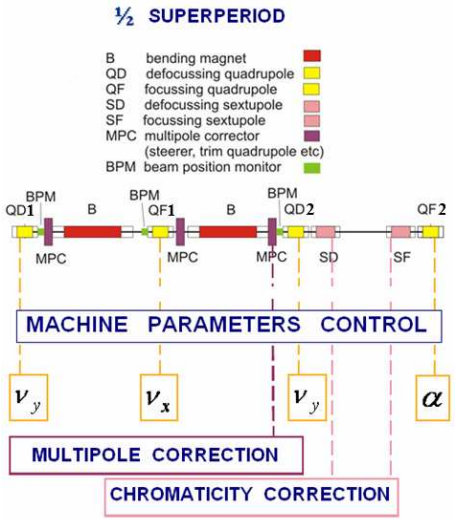

Figure 12: Functional control scheme of elements in a half superperiod

compaction factor on both horizontal and vertical arc tunes, we performed a numerical simulation of such control in the lattice with originally installed maximum possible negative $\alpha = -0.02\,(\gamma_{tr} \approx i7)$.

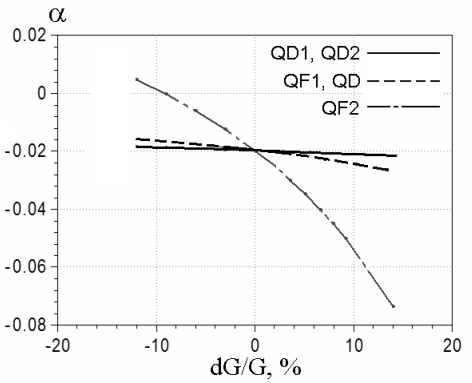

Figure 13: Momentum compaction factor vs quadrupoles gradient

Figure 13 shows how the gradient of quadrupoles QF1, QF2, QD1, QD2 and QD (QD1=QD2) changes the momentum compaction factor in the vicinity of working meaning $\alpha = -0.02$. In the case where QD1=QD2, there is one family of defocusing quadrupoles, and both quadrupoles are feed by one power source.

From these results we can see that the derivatives of momentum compaction factor with a gradient in the quadrupoles are in the relation:

$$\frac{\partial \alpha}{\partial G_{QF2}} >> \frac{\partial \alpha}{\partial G_{QF1}} \approx \frac{\partial \alpha}{\partial G_{QD1}} \approx \frac{\partial \alpha}{\partial G_{QD2}} \qquad (11)$$

Thus, the momentum compaction factor can be very flexibly controlled by the focusing quadrupole QF2 alone. Simultaneously, the QF1 gradient is expected to impact effectively on horizontal tune. Figures 14 and 15 show the numerical simulation of how each family of quadrupoles changes the horizontal and vertical tunes for one half-arc in the vicinity of working points $\nu_{arc\,x} = 2 \times 3.0$ and $\nu_{arc\,y} = 2 \times 3.0$.

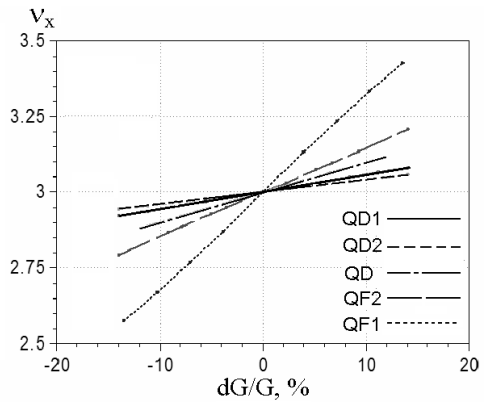

Figure 14: Horizontal tune vs quadrupoles gradient

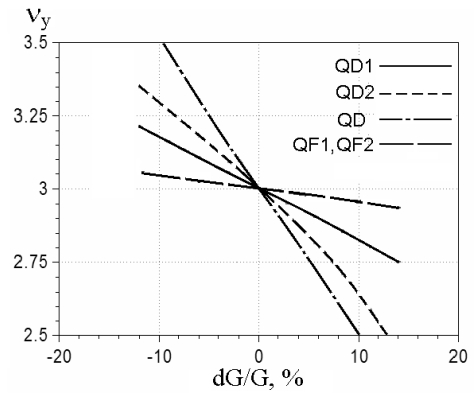

Figure 15 : Vertical tune vs quadrupoles gradient

From these results, we can see that the derivatives of horizontal and vertical tunes with a gradient in the quadrupoles are in the relation:

$$\begin{aligned} \frac{\partial \nu_{arc\,x}}{\partial G_{QF1}} > \frac{\partial \nu_{arc\,x}}{\partial G_{QF2}} >> \frac{\partial \nu_{arc\,x}}{\partial G_{QD1}} \approx \frac{\partial \nu_{arc\,x}}{\partial G_{QD2}} \\ \frac{\partial \nu_{arc\,y}}{\partial G_{QD1}} \approx \frac{\partial \nu_{arc\,y}}{\partial G_{QD2}} >> \frac{\partial \nu_{arc\,y}}{\partial G_{QF1}} \approx \frac{\partial \nu_{arc\,y}}{\partial G_{QF2}} \end{aligned} \qquad (12)$$

After readjusting the momentum compaction factor using the QF2 quadrupole family, the required tunes value $\nu_{arc\,x,y}$ are returned by two-three iteration steps using another quadrupole family QF1 and QD, which in turn weakly influence the momentum compaction factor.

Thus, we have separated internal arc functions:

- momentum compaction factor is controlled by central focusing quadrupole QF2,
- horizontal tune is controlled by focusing quadrupole QF1,
- vertical tune is controlled by defocusing quadrupoles QD1 and QD2 or QD.

Since derivatives $\frac{\partial \nu_{arc\,y}}{\partial G_{QD1}}$ and $\frac{\partial \nu_{arc\,y}}{\partial G_{QD2}}$ have approximately equal values, it is reasonable to use one family of defocusing quadrupoles, QD, only. This allows us to control the vertical tune more easily and more effectively, and does not influence the controllability of other parameters.

CHROMATICITY CORRECTION

The chromaticity is created by the quadrupole and defined as the variation of the betatron tune $\nu_{x,y}$ with the relative momentum deviation $Q'_{x,y} = \frac{d\nu_{x,y}}{d\delta}$, where $\delta = \frac{\Delta p}{p}$. The special optic elements, the sextupoles, are installed into the lattice to correct the chromaticity. Their integrated contribution over the whole ring circumference C on the chromaticity is:

$$\frac{\partial \nu_{x,y}}{\partial \delta} = \pm \frac{1}{4\pi} \int_0^C \beta_{x,y}(s) \cdot D(s) \cdot S(s) ds \qquad (13)$$

Obviously, to strengthen the sextupole efficiency, they have to be allocated in maximum dispersion and with different β_x and β_y values to split the chromaticity correction in the horizontal and vertical planes. With regard to the last point, the "resonant" lattice based on the singlet FODO structure is preferred above other lattices based on doublet or triplet structures. In the "resonant" lattices, the empty space of magnet-free cells is used for the sextupole location (see Fig. 12). In some projects, for instance in JPARC, the focusing sextupole is inserted into the splintered central focusing quadrupole (see Fig. 7). Two families of sextupoles, two focusing and two defocusing sextupoles, are used.

In order to prove independent controllability of chromaticity on both focusing and defocusing sextupoles, we performed a numerical simulation of such control in the lattice with initially installed zero chromaticity $\xi_{x,y} = 0$. Figures 16 and 17 show the numerical simulation results and how the focusing and defocusing sextupoles SF and SD change the horizontal and vertical chromaticity correspondingly. From these results, we can see that the derivatives of horizontal and vertical chromaticities with gradient in the sextupoles can be related as follows:

$$\left|\frac{\partial \xi_x}{\partial G_{SF}}\right| > \left|\frac{\partial \xi_x}{\partial G_{SD}}\right| \quad \text{and} \quad \left|\frac{\partial \xi_y}{\partial G_{SD}}\right| > \left|\frac{\partial \xi_y}{\partial G_{SF}}\right| \qquad (14)$$

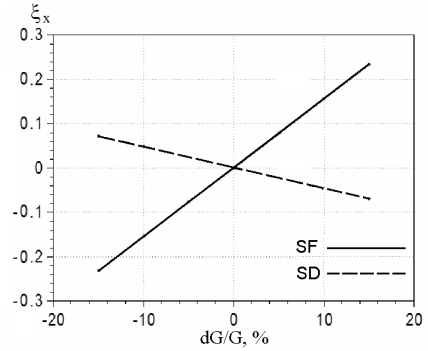

Figure 16: Horizontal chromaticity vs focusing and defocusing sextupole gradient

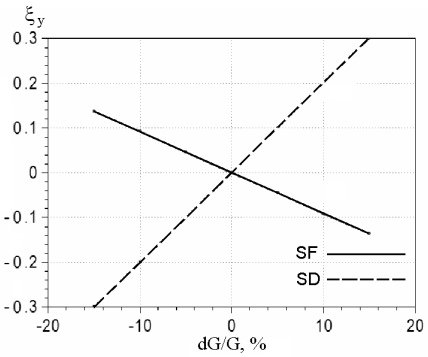

Figure 17: Vertical chromaticity vs defocusing and focusing sextupole gradient

Thus, two sextupole families can control both horizontal and vertical chromaticities independently and successfully.

COMPENSATION OF SEXTUPOLE NONLINEARITY

In the common case, the lattice has nonlinear optics. Usually, the strongest contribution to the nonlinearity is made by the chromatic sextupoles. In order to investigate the nonlinear optics, we use the Hamiltonian formalism. In the variable "action-angle", $I_{x,y}, \vartheta_{x,y}$ coordinates

$$I_x = (1+\delta)\frac{x^2}{2\beta_x(s)}\sec^2\vartheta_x, \quad I_y = (1+\delta)\frac{y^2}{2\beta_y(s)}\sec^2\vartheta_y \tag{15}$$

the Hamiltonian is presented as:

$$H(I_x,\vartheta_x,I_y,\vartheta_y) = \nu_x I_x + \nu_y I_y + \frac{1}{2}\sum_{j,k,l,m} E_{lm}^{jk}\cdot I_x^{j/2}\cdot I_y^{k/2}\exp i(l\vartheta_x + m\vartheta_y), \tag{16}$$

where the coefficients E_{lm}^{jk} depend on the value and distribution of the nonlinear elements, and they have the periodicity 2π with the new "time" coordinate $\theta = \frac{1}{R}\cdot s$:

$$E_{lm}^{jk} = \sum_p h_{jklmp}\exp ip\theta \tag{17}$$

So, the nonlinear part of Hamiltonian is:

$$V = \frac{1}{2}\sum_{j,k,l,m}\sum_{p=-\infty}^{\infty} h_{jklmp}\cdot I_x^{j/2}\cdot I_y^{k/2}\exp i(l\vartheta_x + m\vartheta_y - p\theta) \tag{18}$$

with the Fourier coefficients:

$$h_{jklmp} = \frac{1}{2\pi}\int_0^{2\pi} E_{lm}^{jk}\exp ip\theta\,. \tag{19}$$

In case two conditions are fulfilled, namely the harmonic value $h_{jklmp}\neq 0$ for some of the nonlinear elements M_{j+k}, and $k_x\nu_x + k_y\nu_y = p$, where $k_x = l$ and $k_y = m$, we have nonlinear resonance, and on the contrary, when we wish to exclude the resonance influence, we should minimize the harmonic amplitude h_{jklmp}. The only condition, which cancels all coefficients E_{lm}^{jk} is the zero value of $h_{jklmp}=0$ for all j,k,l,m. In particular, where the chromaticity correction on arcs with S_{arc} superperiods is performed, the sextupoles must be placed with the phase advances μ_x, μ_y per superperiod, when the harmonic is $h_{jklmp}=0$ for all above-mentioned combinations of j,l,k,m in (19), and the total multipole of the third order is canceled:

$$M_3^{total} = \sum_{n=0}^{N} S_{x,y}\beta_x^{l/2}\beta_y^{m/2}\exp in(l\mu_x + m\mu_y) = 0\,, \tag{20}$$

where $S_{x,y}$ are the sextupoles gradient. In the "resonant" lattice, the superperiod number S_{arc} is even and the arc tune ν_{arc} is odd, then the phase advance between similar sextupoles of $n-th$ and $\left(n+\frac{S_{arc}}{2}\right)-th$ superperiods equals $l\cdot\mu_x\cdot\frac{S_{arc}}{2} = l\cdot\frac{2\pi\nu_x}{S_{arc}}\cdot\frac{S_{arc}}{2} = \pi\nu_x l$ (see Fig. 9). In the first order of the perturbation theory, the sextupole excites four resonances $\{l,m\} = \{1,0;\,3,0;\,1,\pm 2\}$. Taking into account that sextupole takes the odd integer l, we have the conditions required to compensate for each sextupole's nonlinear action with another one.

The same can be inferred for the sextupole components in the magnets, since each magnet has its twin located

on $\pi\nu_x l$ phase advance, where the nonlinear kick is compensated.

In case of essential chromaticity contribution from the straight section a method of the second order non-linearity compensation has to be foreseen as well. Solving the nonlinear equation and deriving the Hamiltonian (16) in the first order of the perturbation theory, the value h_{jklmp} is taken as the small parameter, and all non-resonant terms are omitted. Thus, in the first order of the perturbation theory, the sextupoles can be canceled. However, in the second order, the nonlinear perturbation already contains the higher order of h_{jklmp}, which gives nonlinear tune shifts, such as octupoles [10]. In principle, the sextupole nonlinear tune cannot be controlled after the sextupole location has been fixed. Therefore, the sign of total chromaticity is controlled by the octupoles, which are located in the multi-pole correctors. Thus, after chromaticity correction, the nonlinear tune shift is measured and then using the correcting octupole, we adjust the required sign and value of the nonlinear tune shift, as described in [10].

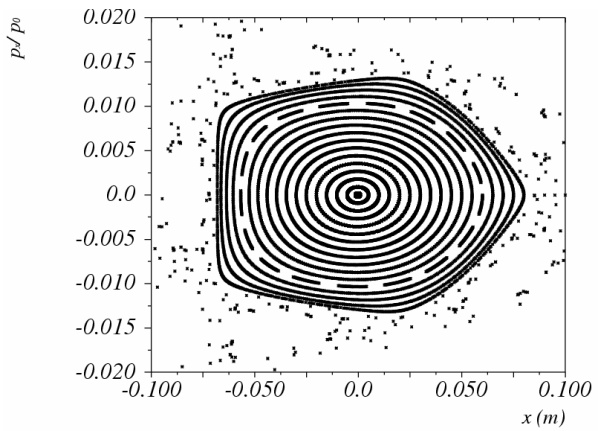

Figure 18: PS2 dynamic aperture after chromaticity correction at Δp/p=1%

After all corrections have been made, we have done the tracking for the maximum momentum spread beam $\Delta p / p = 1\%$. Figure 18 shows the results of dynamic aperture calculations after chromaticity correction. For horizontal plane it is ~600 *mm·mrad* and for vertical plane it has approximately the same meaning ~500 *mm·mrad*.

CONCLUSION

The PS2 imaginary gamma-transition lattice was developed with features:

- ability to achieve the negative momentum compaction factor using the resonantly correlated curvature and gradient modulations;
- gamma transition variation in a wide region from $\gamma_{tr}=\nu_x$ to $\gamma_{tr}=i\nu_x$ with quadrupole strength variation only;
- integer odd 2π phase advance per arc with even number of superperiod and dispersion-free straight section;
- independent optics parameters of arcs and straight sections;
- two families of focusing and one of defocusing quadrupoles;
- separated adjustment of gamma transition, horizontal and vertical tunes;
- convenient chromaticity correction method using sextupoles;
- first-order self-compensating scheme of multipoles and as consequence low sensitivity to multipole errors and a large dynamic aperture

ACKNOWLEDGMENTS

Author is grateful to M. Benedict and E. Shaposhnikova for scientific discussion of specific problems and parameters of the proton synchrotron PS2.

REFERENCES

[1] W. Bartmann, M. Benedikt, C. Carli, B. Goddard, S. Hancock, J.M. Jowett, Y.Papaphilippou, Optics Considerations for the PS2, Proceedings of Particle Accelerator Conference 2007, Albuquerque, p.739, http://accelconf.web.cern.ch/accelconf/p07/PAPERS/TUODKI02.PDF;
W. Bartmann, M. Benedikt, C. Carli, B. Goddard, S. Hancock, J.M. Jowett, A. Koschik, Y. Papaphilippou,http://indico.cern.ch/getFile.py/access?contribId=66&sessionId=16&resId=2&materialId=slides&confId=20082

[2] Yu.Senichev, A «resonant» lattice for a synchrotron with a low or negative momentum compaction factor, submitted in Particle Accelerator, KEK Preprint 97 40, 1997, 27 pages, http://doc.cern.ch/tmp/convert_SCAN-9711073.pdf

[3] N. Golubeva, A. Iliev, Yu. Senichev, The new lattices for the booster of Moscow Kaon Factory, Proceedings of International Seminar on Intermediate Energy Physics, Moscow 1989, vol. 2, p. 290, INR, Moscow, November 1989

[4] U. Wienands, R. Servranckx, N. Golubeva, A. Iliev, Yu. Senichev. A racetrack lattice for the TRIUMF Kaon Factory Booster, Proceedings of the 15-th International Conference on High Energy Accelerators, Hamburg, 1992

[5] E. Courant et al., Low Momentum Compaction Lattice Study for the SSC Low Energy Booster, Proceeding IEEE Particle Accelerator Conference, San Francisco, CA,1991, http://accelconf.web.cern.ch/accelconf/p91/PDF/PAC1991_2829.PDF

[6] H. Schönauer, B. Autin, R. Cappi, J. Gareyte, R. Garoby, M. Giovannozzi, H. Haseroth, M. Martini, E. Métral, W. Pirkl,C.R. Prior, G.H. Rees, RAL, Chilton, Didcot, I. Hofmann, Yu. Senichev, A slow-cycling proton driver for a Neutrino Factory, Proceedings of EPAC, Vienna, 2000, http://accelconf.web.cern.ch/AccelConf/e00/PAPERS/THP2A09.pdf

[7] Y. Ischi, S. Machida, Y. Mori_, S. Shibuya, Lattice design of JHF synchrotrons, Proceedings of APAC, Tsukuba, 1998, http://hadron.kek.jp/jhf/apac98/5D002.pdf

[8] Yu. Senichev, S. An, K. Bongardt, R. Eichhorn, A. Lehrach, R. Maier, S. Martin, D. Prasuhn, H. Stockhorst, R. Toelle, Lattice Design Study for HESR, Proceedings of EPAC, Lucerne, 2004, p.653, http://accelconf.web.cern.ch/accelconf/e04/PAPERS/MOPLT047.PDF

[9] W. Bartmann, M. Benedict, B. Goddard, T. Kramer, A. Koschik, PS2 injection, extraction and beam transfer concepts, Proceedings of PAC 2007, Albuquerque, p.1598, http://accelconf.web.cern.ch/accelconf/p07/PAPERS/TUPAN094.PDF

[10] A. Chechenin, E. Senicheva, R. Maier, Yu. Senichev, The high order non-linear beam dynamics in High Energy Storage Ring of FAIR, Proceedings of EPAC, Edinburg 2006, pp.2083-2085 http://accelconf.web.cern.ch/accelconf/e06/PAPERS/WEPCH072.PDF